Semi-empirical modelling of the electrical behaviour of DC-arc smelting furnaces

by Q.G. Reynolds* and R.T. Jones*

Synopsis

DC arc furnaces are widely used for steel scrap melting, and are increasingly being used for smelting applications as well. The electrical resistivity of slags varies widely, from highly conductive slags in ilmenite smelting, to highly resistive slags in applications such as cobalt recovery from non-ferrous slags, and nickel laterite smelting. Models have been developed to predict the electrical behaviour of the DC open plasma arc and the molten slag bath. These models allow the voltage and current ranges of furnace power supplies to be specified.

Introduction

Direct current arc furnaces have been in use in the metallurgical industry since the late 1800s in the field of steel scrap processing. More recently, they have started gaining acceptance in the area of smelting of ores of many varieties, for example, the smelting of chromite to produce ferrochromium[4], ilmenite smelting to produce titania slag and pig iron[4], recovery of cobalt from non-ferrous smelter slags[2], treatment of stainless-steel plant dust[5], smelting of nickel laterite ore to produce ferronickel[3], and production of platinum group metals[1]. With these new process applications come new challenges to the designer of the DC furnace—one such is the understanding of the electrical behaviour of the furnace in response to process and operational changes, which can allow the process engineer to specify appropriate ranges of voltage and current for the power supply.

It is very important for the power supply of a furnace to be able to deliver power at the designed level, otherwise furnace throughput will be adversely affected. If the actual operating voltage is lower than anticipated, the power supply might be unable to deliver the current required for the intended power. On the other hand, if running a process with a highly resistive slag, the power supply needs to be able to operate at a sufficiently high voltage.

The power supply is often the item with the longest delivery time when building a furnace, so the voltage and current specifications are often needed at a very early stage of a project. As power supplies are very expensive items, one cannot afford to get the specifications wrong.

A simplified schematic of the DC smelting furnace is shown in Figure 1. Of relevance to the electrical design is the circuit formed by the DC power supply, which is typically a bank of rectifiers connected to an AC transformer, and the furnace unit itself. The total load across the unit is seen to consist of two loads in series—the first is the plasma arc column, and the second is the slag bath. Modelling the electrical behaviour of these two components allows the behaviour of the furnace as a whole to be understood, and can feed forward into the design procedure for the power supply of an industrial-scale plant.

Semi-empirical models of furnace electrical behaviour

Electrical model of the arc

In order to have a reasonably complete description of the electrical behaviour of the DC smelting furnace, a model of the behaviour of the arc is essential. Such a model is provided in the work of Ben Bowman[6–8], who correlated a large amount of test data in the range 1–10 kA and verified his relationship against industrial measurements up to 100 kA.

Bowman's equation describes the radius of the conducting volume of the arc as a function of the distance from the cathode attachment spot. The assumptions include an axi-symmetric arc and no interaction effects at the anode. The equation, which stems from a large quantity of data collected in the 1 to 10 kA range, looks as follows:

* *Mintek, Private Bag X3015, Randburg, South Africa.*

 SA ISSN 0038–223X/3.00 + 0.00. Paper received Jan. 2004; revised paper received Apr. 2004.

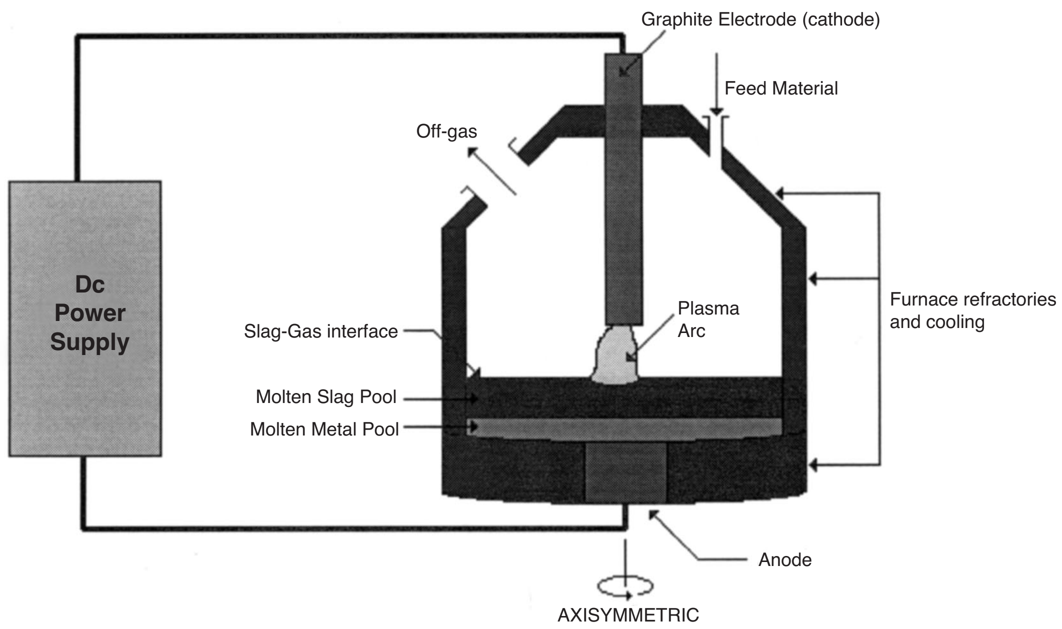

Figure 1—Schematic of a DC smelting furnace

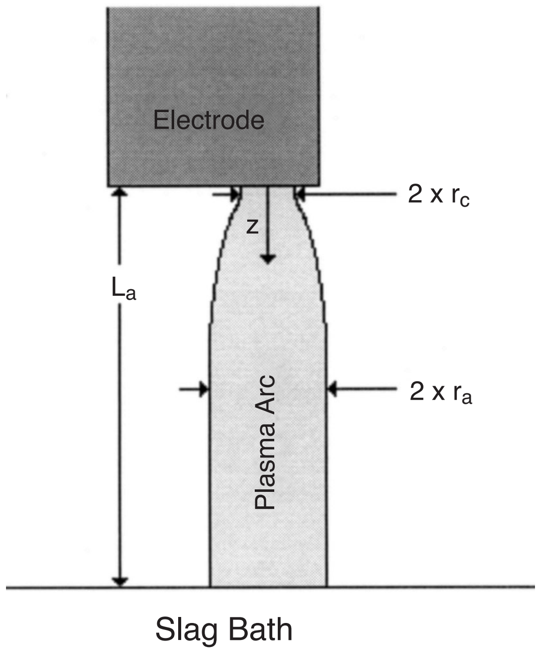

Figure 2—Plasma arc geometry, showing variables used in modelling

$$\frac{r_a}{r_k} = A + B\exp\left(-\frac{z}{5r_k}\right) \qquad [1]$$

Equation [1] shows the functional dependence of the arc radius, r_a, on z, which is the distance from the cathode surface. r_k, the radius of the arc at the cathode surface, is determined by the value of the cathode-spot current density, j_k, estimated by Bowman to be 3.5 kA/cm2. A and B are constants in Bowman's model, with the values of 3.2 and -2.2 respectively.

Assuming a parabolic distribution of electrical conductivity along the arc's radius, the arc shape function allows the arc voltage to be obtained by integration. Several empirical constants of Bowman's, along with a single variable parameter, the average arc resistivity, appear in the arc voltage expression. Variation of the arc resistivity then allows the model to be fitted to pilot or industrial plant data. The integration required is:

$$V = \rho_a.\sqrt{I}.\sqrt{\frac{j_k}{\pi}}.\int\left(\frac{r_k}{r_a}\right)^2 dZ \qquad [2]$$

$$Z = \frac{z}{r_k}$$

Where:

ρ_a = average arc resistivity through conducting section of arc column, Ω cm
I = current, kA
r_a = arc radius, cm (from Equation [1])

The final result of this integration is a nonlinear expression relating the arc's voltage to its length and current. Several examples are shown graphically in Figure 3.

Electrical model of the slag bath

The slag bath in a DC smelting furnace typically behaves as an ohmic conductor, unlike the arc which is extremely non-linear. To model the bath's electrical behaviour with a fair degree of accuracy, a two-dimensional axisymmetric numerical model is used which describes the variation of the potential (voltage) through the bath. The model operates by solving Laplace's equation for potential.

$$\frac{1}{r}\frac{\partial}{\partial r}r\frac{\partial V}{\partial r} + \frac{\partial^2 V}{\partial z^2} = 0 \qquad [3]$$

This partial differential equation governs the potential distribution in a material of uniform electrical conductivity, and is solved numerically using a finite-volume method on a non-uniform mesh. Details of the general numerical method used can be found in Reference 10. The geometry used is shown in Figure 4.

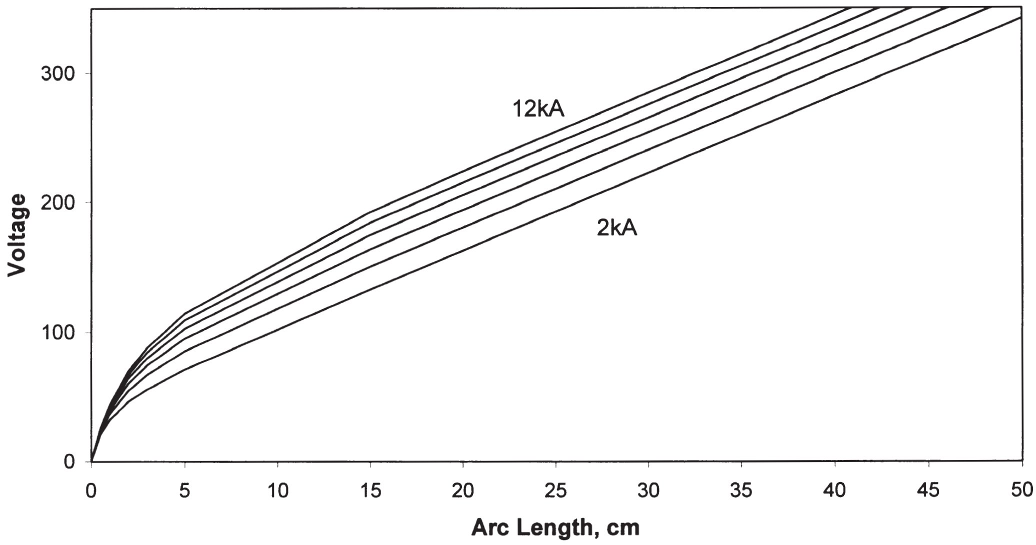

Figure 3—Graph showing variation of arc voltage with current and arc length according to Bowman model (examples shown are for ρ_a=0.0175 Ω cm)

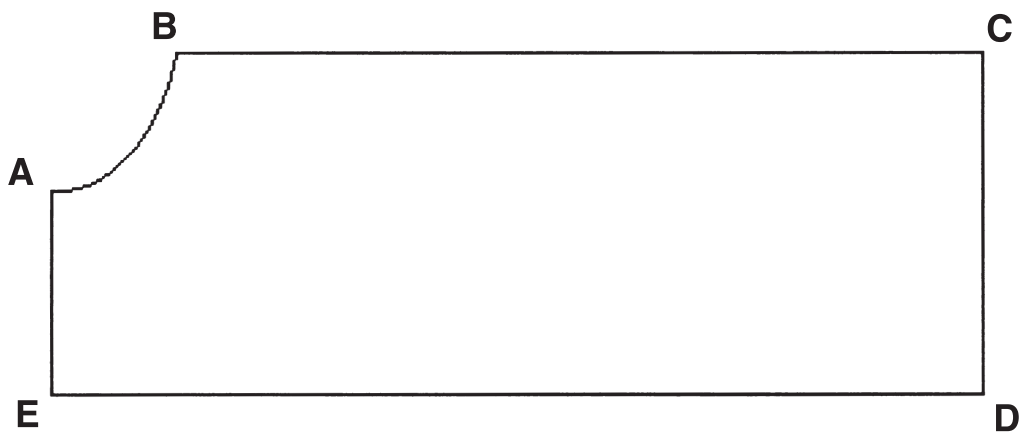

Figure 4—Geometry of axisymmetric furnace bath

The section A-B is parabolic in shape, representing the zone in which the plasma arc attaches electrically to the surface of the slag, and the physical depression formed by the impinging plasma gases. The current (specified in the model) is applied as a potential-gradient boundary condition across this surface. The section B-C is the upper surface of the liquid bath and is taken to be electrically insulating. The section C-D is the furnace wall, also assumed to be electrically insulating. D-E is the interface between the metal pool and the slag bath, which is taken to be at ground or anode voltage, V=0. E-A is the centerline of the furnace.

In order to calculate the dimensions of the arc attachment depression, an empirical correlation given by Maecker[6] for the thrust generated by an electromagnetic arc as a function of its current is used. Since the potential-theory model uses a parabolic shape to represent the depression generated by the arc jet, its volume and hence mass of slag displaced may be easily calculated and equated to the impinging thrust force. This gives a relationship between the diameter and depth of the depression at a given current, effectively eliminating one parameter. The remaining parameter is able to be calculated if one knows the approximate ratio of diameter to depth for the depression. This ratio has been determined via extensive photographic work conducted at Mintek[9] to be of the order of 6:1.

This ratio is fairly pivotal in the behaviour of the potential theory model of the slag bath, and as it is a largely empirical number, some further comments are justified. The shape of the depression is affected by two factors—the hydrodynamic stability of the liquid slag in which it is formed, and the motion of the plasma arc. A large body of experimental and theoretical work exists in the field of gas jets impinging on liquid surfaces[11], and all of this work suggests that a ratio less than 1:1 for the depression shape would be unsustainable. In addition, the fact that the arc itself is constantly in very rapid motion over the surface of the slag means that the thrust it produces is 'smeared' over a larger area than just the diameter of the jet. The number of 6:1 provides a good empirical fit to the electrical data while remaining consistent with both the theoretical understanding of arc and gas jet behaviour and the photographic evidence gathered on pilot furnaces operating in the range of 1–10 kA.

Video photography of arcs in much larger furnaces (50–80 kA) suggests qualitatively similar behaviour to furnaces of smaller size, lending support to the idea that the 6:1 ratio may be consistent over a large range of scales.

A simple analysis of the sensitivity of the models to the diameter to depth ratio for an example furnace is shown in Figure 5.

Non-ohmic behaviour of the DC-arc furnace

The design of DC power supplies for the steel melting industry often makes use of the assumption that the furnace has an approximately constant resistance. This of course leads to a directly proportional relationship between voltage and current. In traditional circuit models, the DC arc is also often presented as a constant-voltage device, showing no dependence on current at all. In contrast to this, our modelling and experimental work has shown that a DC smelting furnace is a more nonlinear type of conductor. Figure 6 shows the relationship between voltage and current for a range of different arc lengths according to the models developed above.

Data gathering and analysis

Arc characteristic tests

On a pilot plant furnace, arc characteristic tests are typically performed by measuring the system voltage with the power on, and with the electrode at various known heights above the surface of the slag bath. The test may be performed with feed on or off, and shows the behaviour of the voltage drop in the electric arc as a function of its length. Typical precision for measurements of the electrode position are of the order of one to two millimetres on our control systems, and as a potential source of error is negligible.

Analysis of data from such a test is possible in terms of Equation [2], if one assumes an average representative arc resistivity ρ_a for the arc plasma. The full equation for voltage is somewhat ungainly, and is presented in Equation [4].

$$V_a = \frac{I\rho_a}{m\pi}\left[\begin{array}{l} -\dfrac{1}{a^2+ab}+\dfrac{1}{a^2+ab.\exp(mL_a)}+ \\ \dfrac{\ln(a+b)}{a^2}+\dfrac{mL_a}{a^2}-\dfrac{\ln\left[a+b.\exp(mL_a)\right]}{a^2} \end{array}\right] \qquad [4]$$

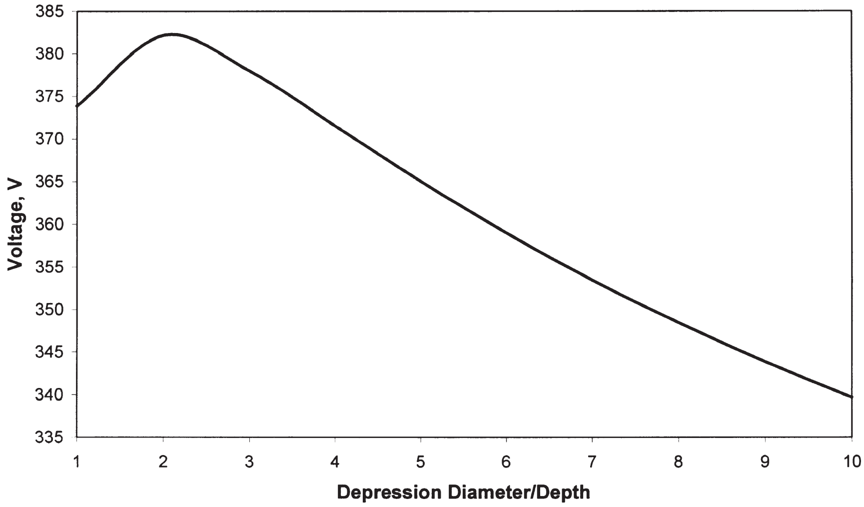

Figure 5—Plot of furnace voltage vs. depression shape ratio for an example pilot-scale DC-arc furnace (5 kA current, 2 m internal diameter, 30 cm slag depth, 20 cm arc length, 1.0 Ω cm slag resistivity, and 0.0175 Ω cm arc resistivity)

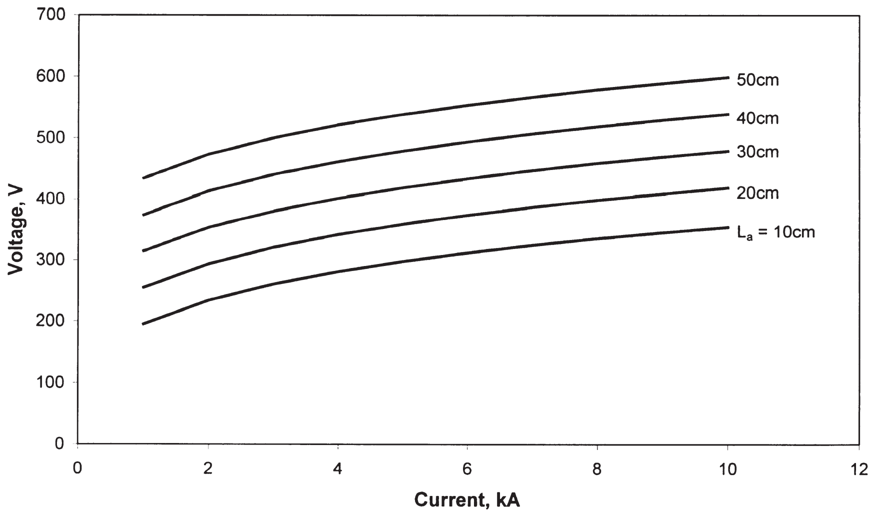

Figure 6—Plot of furnace voltage vs. current for an example pilot-scale DC-arc furnace (2 m internal diameter, 30 cm slag depth, 1.0 Ω cm slag resistivity, and 0.0175 Ω cm arc resistivity)

$$a = Ar_k \tag{4a}$$

$$b = Br_k \tag{4b}$$

$$m = -\frac{1}{5r_k} \tag{4c}$$

The interesting features of the equation are that it has a nonlinear initial portion followed by linear behaviour as the arc length L_a increases. Since L_a and r_k are positive, the asymptotic relationship between arc length and voltage as L_a becomes large is more amenable to analysis, and is:

$$V_{a,L_a\to\infty} = \frac{I\rho_a}{m\pi}\left[\begin{array}{c} -\dfrac{1}{a^2+ab}+\dfrac{1}{a^2}+\dfrac{\ln(a+b)}{a^2}+ \\ \dfrac{mL_a}{a^2}-\dfrac{\ln(a)}{a^2} \end{array}\right] \tag{5}$$

Taking the derivative of this expression gives the asymptotic slope of a voltage - arc length diagram, which is seen to be:

$$\left.\frac{dV_a}{dL_a}\right|_{L_a\to\infty} = \frac{I\rho_a}{\pi a^2} \tag{6}$$

Following from the definition of a and r_k, this simplifies to:

$$\left.\frac{dV_a}{dL_a}\right|_{L_a\to\infty} = \frac{\rho_a j_k}{A^2} \tag{7}$$

Since the arc tests performed at Mintek are carried out at constant current, the bath voltage (which is primarily a function of current-determined geometry) can be taken as constant for the duration of a test. Thus the asymptotic slope will be unaffected by whether the value plotted is the total voltage or the arc voltage, and the plasma resistivity for a particular process or condition may be calculated directly by the fitting of a straight line to the measured data above a certain arc length (see Figure 7).

Slag dip tests

For information concerning the model for the slag bath, one or more sets of slag dip data are generated on the pilot-scale experiment by immersing the electrode into the slag layer to a known depth, with power on. Voltage at a range of immersion depths is then recorded. Since there is no arc present, and the geometry of both the end of the electrode and the slag bath is generally known, analysis using the numerical potential-theory solver described above (with slight modifications to the geometry A-B in Figure 4) is possible to permit calculation of the electrical resistivity, ρ_b, of the slag.

An example of such an analysis is shown in Figure 8. This test was conducted on a process treating waste reverbatory furnace slags for environmental clean-up and the production of cobalt.

Knowing the slag resistivity allows the calculation of the bath voltage in an arcing scenario, from:

$$V_b = \rho_b I K_C \tag{8}$$

Here, K_C is the cell constant of the system, a parameter that includes all geometric effects contributing to the variation in potential across the furnace slag bath. K_C is calculated using the numerical potential-theory model, and multiplied by the slag resistivity and current in order to give the bath voltage for a particular scenario.

Scale-up for design of industrial plants

Once the various arc and slag resistivities for a particular process are available, either via the testing described above or from other sources, the electrical models may be used to design the power supply required for industrial-scale operation.

This is done as follows. The relevant variables in the electrical models for the operation of the furnace are the power, total voltage, current, and arc length. In our models, specifying the current and arc length (with all other physical properties and dimensions known) allows the calculation of

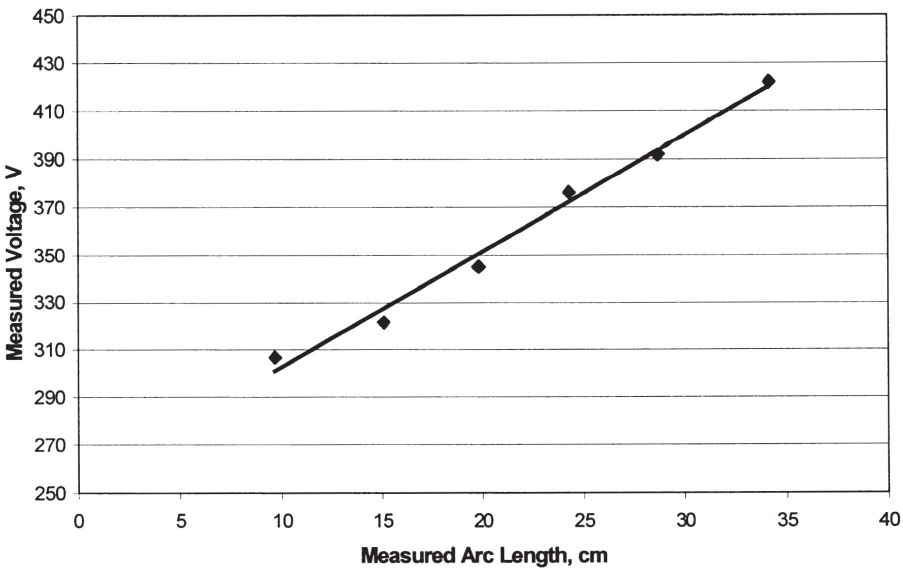

Figure 7—Graph showing analysis of a set of arc test data (points) by fitting the Bowman arc model (solid line)

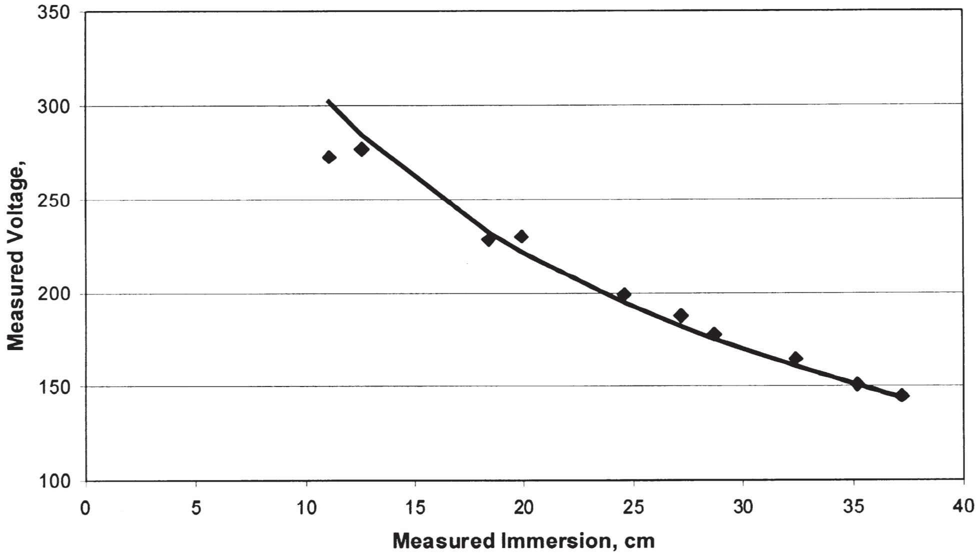

Figure 8—Graph showing analysis of a set of slag dip test data (points) by fitting the potential-theory model (solid line)

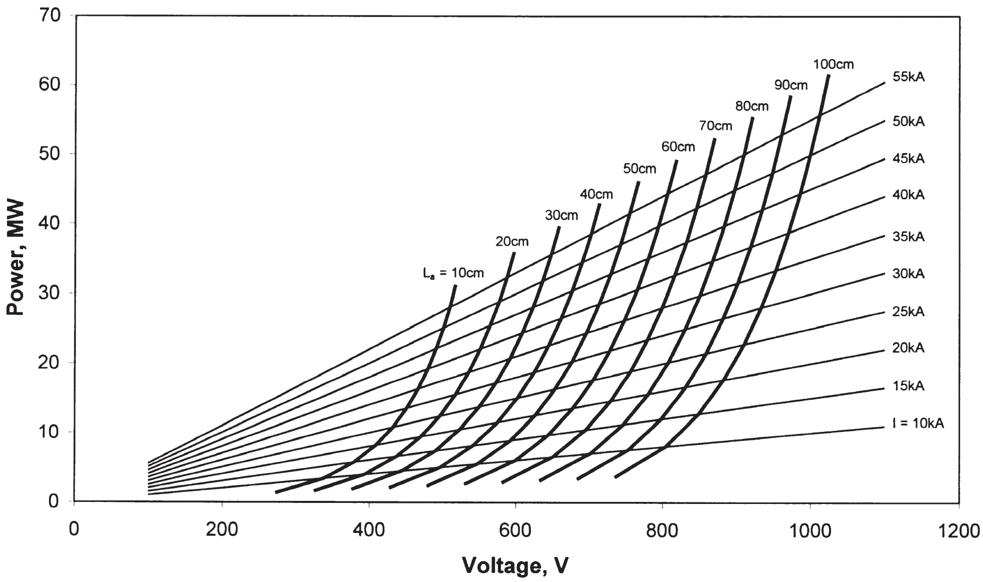

Figure 9—P V design plot for an example DC arc furnace (10 m internal diameter, 50 cm slag depth, 1.0 Ω cm slag resistivity, and 0.015 Ω cm arc resistivity)

the total voltage across the furnace and hence the total power dissipated in the unit. DC power supplies are generally specified based on the power and voltage they are expected to deliver, so in order to produce data of some use to the electrical design engineer, the relationship $(P, V) = f(I, L_a)$ needs to be inverted and presented as $(I, L_a) = f^{-1}(P, V)$.

For current, this is simple, due to the relationship:

$$P = VI$$
$$I = \frac{P}{V} \qquad [9]$$

For arc length, it is somewhat more complicated. At constant L_a, we have:

$$V_a = f_1(I)$$
$$V_b = f_2(I) \qquad [10]$$

where f_1 is the Bowman arc voltage model, and f_2 is the potential-theory model of the slag bath. Current appears in the latter as the geometry of the arc attachment zone is dependent on arc thrust, and hence furnace current.

Total furnace voltage and power at constant arc length are thus seen to be parameterized by current:

$$V = f_1(I) + f_2(I)$$
$$P = \left[f_1(I) + f_2(I)\right]I \qquad [11]$$

These two relationships permit the plotting of a power vs. voltage graph. Figure 9 shows an example of one such plot.

For a real industrial design, uncertainties in many of the 'constant' variables such as slag depth and the various resistivities will generally result in several of the above diagrams being drawn. This enables best- and worst-case scenarios to be considered for the design specification of the power supply to be used on the furnace.

Conclusion

Several semi-empirical models for understanding the electrical behaviour of DC smelting furnaces on the pilot and industrial scales have been presented here. These models are in constant use at Mintek, and continue to be refined as they are used for an ever wider variety of smelting processes and furnace designs.

The models extend naturally to scale-up calculations once sufficient data has been gathered on the pilot scale. This facilitates the specification of the DC power supply for the industrial-scale plant.

References

1. JONES, R.T. ConRoast:- DC arc smelting of dead-roasted sulphide concentrates, *Third International Sulfide Smelting Symposium* (*Sulfide Smelting '02*), Seattle, Washington, USA, 2002, pp. 435–456. http://www.mintek.co.za/Pyromet/Files/ConRoast.pdf
2. JONES, R.T., DENTON, G.M., REYNOLDS, Q.G., PARKER, J.A.L., and VAN TONDER, G.J.J. Recovery of cobalt from slag in a DC arc furnace at Chambishi, Zambia, *Journal of the South African Institute of Mining and Metallurgy*, Jan/Feb 2002, pp. 5–9. http://www.mintek.co.za/Pyromet/Chambishi/Chambishi.htm
3. LAGENDIJK, H., and JONES, R.T. Production of Ferronickel from Nickel Laterites in a DC-Arc Furnace, *36th Annual Conference of Metallurgists*, Sudbury, Canada, August 1997, pp. http://www.mintek.co.za/Pyromet/Laterite/Laterite.htm
4. JONES, R.T., BARCZA, N.A., and CURR, T. Plasma Developments in Africa, *2nd International Plasma Symposium*: *World Progress in Plasma Applications*, Palo Alto, California, 9–11 February 1993, pp. http://www.mintek.co.za/Pyromet/Plasma/Plasma.htm
5. SCHOUKENS, A.F.S., SHAW, F., and CHEMALY, E.C. The Enviroplas process for the treatment of steel-plant dusts, *Journal of the South African Institute of Mining and Metallurgy*, January 1993, pp. 1–7. http://www.mintek.co.za/Pyromet/Files/1993EnviroplasDust.pdf
6. BOWMAN, B. Convective heat transfer and power balance in high current free-burning arcs, *Electrowarme International 30* (1972) B2 April, pp. B87–B93.
7. JORDAN, G.R., BOWMAN, B., and WAKELAM, D. Electrical and photographic measurements of high-power arcs, *Journal of Physics D*: *Applied Physics*, vol. 3, 1970, pp. 1089–1099.
8. BOWMAN, B. Properties of Arcs in DC Furnaces, 1994 *Electric Furnace Conference proceedings*, pp. 111–120.
9. JONES, R.T., REYNOLDS, Q.G., and ALPORT, M.J. DC Arc Photography and Modelling, *Minerals Engineering*, vol. 15, issue 11S1, 2002, pp. 985–991.
10. PATANKAR, S.V. *Numerical Heat Transfer and Fluid Flow*, Hemisphere Publishing Corporation, 1980.
11. CHESLAK, F.R., NICHOLLS, J.A., and SICHEL, M. Cavities formed on liquid surfaces by impinging gaseous jets, *Journal of Fluid Mechanics* (1969), vol. 36, part 1, pp. 55–63. ◆